922 *Chem. Mater.* **2010,** *22,* 922–927
DOI:10.1021/cm901762h

CHEMISTRY OF MATERIALS
Article

CdS/CdSe Co-Sensitized TiO_2 Photoelectrode for Efficient Hydrogen Generation in a Photoelectrochemical Cell†

Yuh-Lang Lee,* Ching-Fa Chi, and Shih-Yi Liau

Department of Chemical Engineering, National Cheng Kung University, Tainan 70101, Taiwan

Received June 24, 2009. Revised Manuscript Received August 18, 2009

An efficient photoelectrode is prepared by sequentially assembled CdS and CdSe quantum dots (QDs) onto a nanocrystalline TiO_2 film. The CdS/CdSe co-sensitized photoelectrode was found to have a complementary effect in the light absorption. Furthermore, the cascade structure, TiO_2/CdS/CdSe, exhibits a significant enhancement in the current−voltage response, both in dark conditions and under light illumination. On the contrary, the performance of the reverse structure, TiO_2/CdSe/CdS, is much less than the electrode using a single sensitizer. The open circuit potentials measured in the dark for these electrodes indicates that a Fermi level alignment occurs between CdS and CdSe after their contact, causing downward and upward shifts of the band edges, respectively, for CdS and CdSe. A stepwise band edge structure is, therefore, constructed in the TiO_2/CdS/CdSe electrode, which is responsible for the performance enhancement of this photoelectrode. The saturated photocurrent achieved by the TiO_2/CdS/CdSe electrode under the illumination of UV cutoff AM1.5 (100 mW/cm^2) is 14.9 mA/cm^2, which is three times the value obtained by the TiO_2/CdS and TiO_2/CdSe electrode. When a ZnS layer is further deposited for passivating the QDs, the corresponding hydrogen evolution rate measured for the TiO_2/CdS/CdSe/ZnS electrode is 220 μmol/(cm^2 h) (5.4 mL/(cm^2 h)). This performance is presently the highest reported for the QD-sensitized photoelectrochemical cells.

Introduction

Hydrogen is considered to be a potential candidate for a nonpolluting energy source due to its environmental friendly and renewable characteristics. Since the innovative report published in 1972 for photoelectrochemical water splitting using titanium dioxide (TiO_2) photoelectrodes,[1] many studies have been dedicated to the development of photocatalytic materials or photoelectrochemical cells for conversing solar energy into hydrogen.[2−5] Although TiO_2 is one of the most important materials widely investigated for use in photocatalysis, photoelectrodes, and solar cells, the wide bandgap (3.2 eV) of TiO_2 limits its photocatalytic property in the UV region. To extend the activity of a photoelectrode into the visible light region, various approaches were employed including doping TiO_2 with other impurities[6−8] and sensitization of TiO_2 with semiconductors which absorb light in the visible region.

Semiconductor quantum dots (QDs) such as CdS,[9−11] CdSe,[12] PbS,[13,14] PbSe,[15] and InP[16] have been assembled on porous TiO_2 films as sensitizers of photoelectrodes. Among these, cadmium sulfide (CdS) and cadmium selenide (CdSe) are more promising materials reported to have better performance. Peng and co-workers reported an efficiency of 4.15% for an electrochemical cell using a CdS-QDs sensitized TiO_2 nanotube array photoelectrode.[17] On the basis of a TiO_2 inverse opal, Diguna at al.[18] prepared a CdSe sensitized solar cell with an energy conversion efficiency of 2.7%. In our previous work, CdS QDs were assembled onto a mesoscopic TiO_2 film using a chemical bath deposition (CBD) process performed in alcohol solutions.[19] This modified

† Accepted as part of the 2010 "Materials Chemistry of Energy Conversion Special Issue".

*Corresponding author. E-mail: yllee@mail.ncku.edu.tw. Tel: 886-6-2757575 ext 62693. Fax: 886-6-2344496.

(1) Fujishima, A.; Honda, K. *Nature* **1972**, *238*, 37.
(2) Kazuhiko, M.; Kazunari, D. *J. Phys. Chem. C* **2007**, *111*, 7851.
(3) Kato, H.; Asakura, K.; Kudo, A. *J. Am. Chem. Soc.* **2003**, *125*, 3082.
(4) Wang, Y.; Zhang, Z.; Zhu, Y.; Li, Z.; Vajtai, R.; Ci, L.; Ajayan, P. M. *ACS Nano* **2008**, *2*, 1492.
(5) Maeda, K.; Takata, T.; Hara, M.; Saito, N.; Inoue, Y.; Kobayashi, H.; Domen, K. *J. Am. Chem. Soc.* **2005**, *127*, 8286.
(6) Asahi, R.; Morikawa, T.; Ohwaki, T.; Aoki, K.; Taga, Y. *Science* **2001**, *293*, 269.
(7) Mohapatra, S. K.; Misra, M.; Mahajan, V. K.; Raja, L. S. *J. Phys. Chem. C* **2007**, *111*, 8677.
(8) Khan, S. U. M.; Al-Shahry, M.; Ingler, W. B., Jr. *Science* **2002**, *297*, 2243.
(9) Peter, L. M.; Riley, D. J.; Tull, E. J.; Wijayantha, K. G. U. *Chem. Commun.* **2002**, *10*, 1030.
(10) Lin, S. C.; Lee, Y. L.; Chang, C. H.; Shen, Y. J.; Yang, Y. M. *Appl. Phys. Lett.* **2007**, *90*, 143517.
(11) Robel, I.; Subramanian, V.; Kuno, M.; Kamat, P. V. *J. Am. Chem. Soc.* **2006**, *128*, 2385.
(12) Lee, Y. L.; Huang, B. M.; Chien, H. T. *Chem. Mater.* **2008**, *20*, 6903.
(13) Plass, R.; Serge, P.; Krüger, J.; Grätzel, M. *J. Phys. Chem. B* **2002**, *106*, 7578.
(14) Hoyer, P.; Könenkamp, R. *Appl. Phys. Lett.* **1995**, *66*, 349.
(15) Schaller, R. D.; Klimov, V. I. *Phys. Rev. Lett.* **2004**, *92*, 186601.
(16) Zaban, A.; Micici, O. I.; Gregg, B. A.; Nozik, A. J. *Langmuir* **1998**, *14*, 3153.
(17) Sun, W. T.; Yu, Y.; Pan, H. Y.; Gao, X. F.; Chen, Q.; Peng, L. M. *J. Am. Chem. Soc.* **2008**, *130*, 1124.
(18) Diguna, L. J.; Shen, Q.; Kobayashi, J.; Toyoda, T. *Appl. Phys. Lett.* **2007**, *91*, 023116.
(19) Chang, C. H.; Lee, Y. L. *Appl. Phys. Lett.* **2007**, *91*, 053503.

Published on Web 09/16/2009

Scheme 1. (a) Relative Energy Levels of TiO_2, CdS, and CdSe in Bulk Phase[19] and (b) Ideal Stepwise Band Edge Structure for Efficient Transport of the Excited Electrons and Holes in a CdS/CdSe Co-Sensitized Electrode

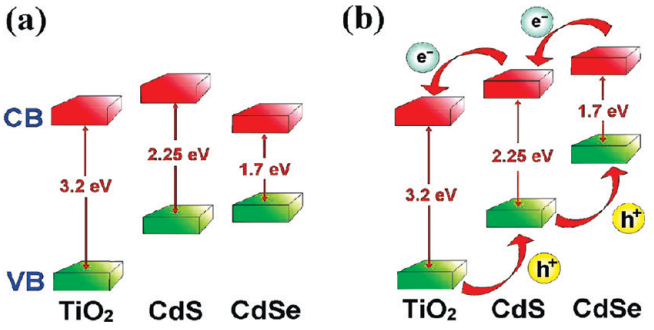

CBD method has proved to be efficient for assembling CdS-QDs into a TiO_2 mesoporous film, and an efficiency of 3.67% was achieved under visible light illumination.[20]

Comparing between CdS and CdSe, CdS has a higher conduction band edge with respect to that of TiO_2,[21] which is advantageous to the injection of excited electrons from CdS (Scheme 1a). However, the band gap of CdS (2.25 eV in bulk) limits its absorption range below the wavelength of approximately 550 nm. On the contrary, although CdSe has a wider absorption range (below ca.730 nm), the electron injection efficiency is less than CdS because its conduction band edge is located below that of TiO_2. To take both advantages of the two materials, CdS and CdSe were used as co-sensitizers of a TiO_2 film in our previous work.[22] The two materials were sequentially assembled onto a TiO_2 film, forming cascade co-sensitized photoelectrodes for QD-sensitized solar cells (QDSSC) application. A history efficiency as high as 4.22% was achieved for the TiO_2/CdS/CdSe photoelectrode.[23] However, a poor performance was obtained for the reversed structure, TiO_2/CdSe/CdS. Fermi-level alignment between CdS and CdSe was proposed to construct a stepwise structure of band-edge levels in the TiO_2/CdS/CdSe electrode (Scheme 1b), which contributes to the high performance of the electrode. Although this inference seems to be reasonable, no direct evidence was given for that model.

In this work, the co-sensitized electrodes were characterized to confirm the cascade structure of CdS and CdSe, as well as the band edge reorganization between CdS and CdSe. These electrodes are further utilized for hydrogen generation in a photoelectrochemical cell. The effectiveness of this co-sensitized electrode is also confirmed in the application of water splitting.

Experimental Section

In-doped tin oxide (ITO, about 7 Ω/sq, Solaronix SA) is used as transparent conducting oxide (TCO) substrates for preparing TiO_2 films. Mesoscopic TiO_2 films were prepared by spin coating of TiO_2 paste (Degussa P25) on ITO substrates, followed by sintering at 450 °C for 30 min. The thickness of a TiO_2 film was controlled by repeated spin-coatings of the TiO_2 layers and measured from the cross sectional image of a scanning electron microscope. In the present study, the thickness of the TiO_2 film is measured to be 12 μm.

Chemical bath deposition (CBD) is used to assemble CdS and CdSe onto a TiO_2 film. For CdS QDs, the CBD method resembles the procedure described in a previous paper.[19,20] A TiO_2 film was dipped into a 0.5 M $Cd(NO_3)_2$ ethanol solution for 5 min, rinsed with ethanol, and then dipped for another 5 min into a 0.5 M Na_2S methanol solution and rinsed again with methanol. The two-step dipping procedure is termed of one CBD cycle, and the incorporated amount of CdS can be increased by repeating the assembly cycles. For CdSe QDs, sodium selenosulphate (Na_2SeSO_3) is used as the Se source for CBD. The Na_2SeSO_3 aqueous solution was prepared by refluxing 0.3 M Se in 0.6 M Na_2SO_3 at 70 °C for about 6 h. The CBD process of CdSe is similar to that of CdS except that a longer time (ca. 1 h) and a higher temperature (50 °C) are required for dipping the sample in the Na_2SeSO_3 solution.

The specimen for TEM observation was prepared using focused ion beam (FIB, SMI 3050) bombardment. A thin lamella was cut out from the cross section of the TiO_2/CdS/CdSe electrode and transferred onto a Cu grid. High-resolution transmission electron microscopy (HR-TEM, JEOL JEM-2100) was operated at 200 kV to observe the crystallinity and arrangement of TiO_2, CdS, and CdSe.

Photoelectrochemical measurement was carried out in a solution containing 0.35 M Na_2SO_3 and 0.24 M Na_2S (pH = 11.5). The solution was purged by argon to remove the dissolved oxygen before experiment. A 300 W Xe lamp (Newport) equipped an AM 1.5G filter was used as the light source. The light was passed through an optical filter, which allowed only wavelengths higher than 400 nm to illuminate the photoanode. The intensity of the incident light was measured with a digital powermeter and was controlled at 100 mW/cm^2. Photocurrent of the working electrode was measured with a potentiostat (CH Instrument, model 611B) at a scan rate of 5 mV/s. The working area of the electrode is 1.0 cm^2, and a Pt wire and a saturated Ag/AgCl electrode were used as the counter and reference electrodes, respectively. The capacitance of the electrode−electrolyte interface at various electrodes was measured by using a potentiostat/galvanostat (Eco Chemie Autolab). All measurements were carried out with AC amplitude of 10 mV in the dark. In the photoelectrochemical cell, the hydrogen was evolved from the Pt electrode and collected in a sealed glass tube. This collected gas was analyzed using a gas chromatograph equipped with a thermal conductivity detector.

Results and Discussion

Light absorption properties of the QD-sensitized TiO_2 electrodes are evaluated using a UV−vis spectrometer. The incorporated amount of CdS or CdSe on a TiO_2 film increases with increasing CBD cycles as the results shown in previous works.[10,20,23] The effect of the CBD layers on the performance of the QD-modified electrodes has been carefully studied in this work, and the optimal layers found for the CdS- and CdSe-sensitized electrodes are all about four layers. For the CdS/CdSe co-sensitized system, the electrode prepared by four layers of CdS plus three layers of CdSe appears to have the best performance. The UV−vis absorption spectra of these electrodes with the optimal CBD layers,

(20) Chi, C. F.; Lee, Y. L.; Weng, H. S. *Nanotechnology* **2008**, *19*, 125704.
(21) Grätzel, M. *Nature* **2001**, *414*, 338.
(22) Lee, Y. L; Lo, Y. S. *Adv. Funct. Mater.* **2009**, *19*, 604.
(23) Shen, Y. J.; Lee, Y. L. *Nanotechnology* **2008**, *19*, 045602.

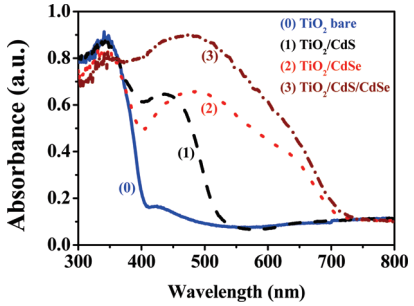

Figure 1. UV−vis absorption spectra of a bare TiO_2 film and the TiO_2 films sensitized by CdS, CdSe, or CdS/CdSe QDs.

as well as a bare TiO_2 film, are shown in Figure 1. The absorption edges of the TiO_2/CdS and TiO_2/CdSe electrodes appear at about 520 and 705 nm, respectively, with similar absorbance at the excitonic peaks. For the co-sensitized electrodes (TiO_2/CdS/CdSe and TiO_2/CdSe/CdS), the absorption edge resembles that of CdSe-modified electrode, but the absorbance is higher than that of TiO_2/CdS or TiO_2/CdSe. Apparently, the co-sensitized electrodes have complementary and enhancement effects in the light harvest. The size of a QD assembled on a TiO_2 film can be estimated from the UV−vis spectra. According to the empirical equations given by Henglein at al.[24] and Yu et al.,[25] the mean diameters of CdS and CdSe QDs were measured to be 10.5 and 6.9 nm, respectively.

To characterize the arrangement of CdS and CdSe on the internal surface of mesoporous TiO_2 film by transmission electron microscopy (TEM), a thin lamella was cut out from the cross section of the TiO_2/CdS/CdSe electrode using focused ion beam (FIB). The bright field TEM image of this specimen clearly indicates a mesoporous structure of the TiO_2 matrix (Figure 2a). The pore sizes measured from this image are about 20 to 40 nm. When the imaging was focused around the matrix/pore interface, various crystalline planes were clearly observed (Figure 2b). The larger crystallite appearing in the left region of Figure 2b is identified to be TiO_2. The lattice spacing measured for this crystalline plane is 0.352 nm, corresponding to the (101) plane of anatase TiO_2 (JCPDS 21-1272). Around the TiO_2 crystallite, fine crystallites with various orientations and lattice spacing were observed. By carefully measuring the lattice parameters and comparing with the data in JCPD, the crystallites connecting to the TiO_2 are CdS, and CdSe locates outside by the CdS (Figure 2b). Therefore, the cascade structure of CdS/CdSe assembled on the TiO_2 surface was confirmed by the HR-TEM image. The TEM image also indicates that the CdS and CdSe are presented in a polycrystalline structure. The sizes of CdS and CdSe crystallites range between 4 to 10 nm, consistent with the sizes evaluated from the UV−vis spectrum.

Figure 3 shows the current density versus potential ($I-V$) curves for the QD-sensitized TiO_2 electrodes measured in dark conditions or under light illumination. For

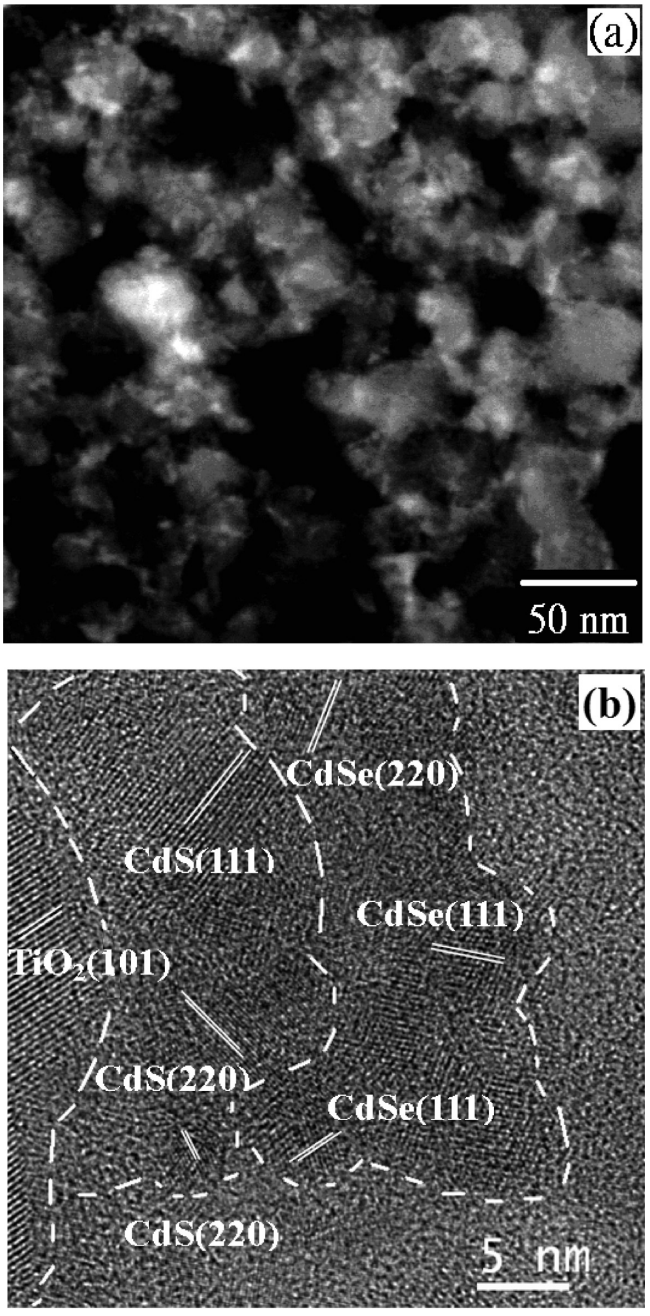

Figure 2. High-resolution TEM images showing a mesoporous structure of the TiO_2/CdS/CdSe electrode (a) and the arrangement of CdS and CdSe around a TiO_2 crystallite (b).

the $I-V$ curve measured in the dark (Figure 3a), the current response of these electrodes at positive bias increases in the order: TiO_2/CdSe ≈ TiO_2/CdSe/CdS < TiO_2/CdS < TiO_2/CdS/CdSe, indicating that the TiO_2/CdS/CdSe electrode has a band edge structure with superior ability for charge transfer. On the other hand, the charge transfer in the reverse structure, TiO_2/CdSe/CdS, has a relatively higher resistance. For an n-type semiconductor such as CdS or CdSe, the charge transfer in the dark is dominated by the majority carrier (electron) through the conduction band. The present result suggests that a stepwise conduction band edge was constructed in the TiO_2/CdS/CdSe electrode. Since the position of the conduction band of CdSe was reported to locate below

(24) Spanhel, L; Haase, M; Weller, H; Henglein, A. *J. Am. Chem. Soc.* **1987**, *109*, 5649.
(25) Yu, W. W.; Qu, L.; Guo, W.; Peng, X. *Chem. Mater.* **2003**, *15*, 2854.

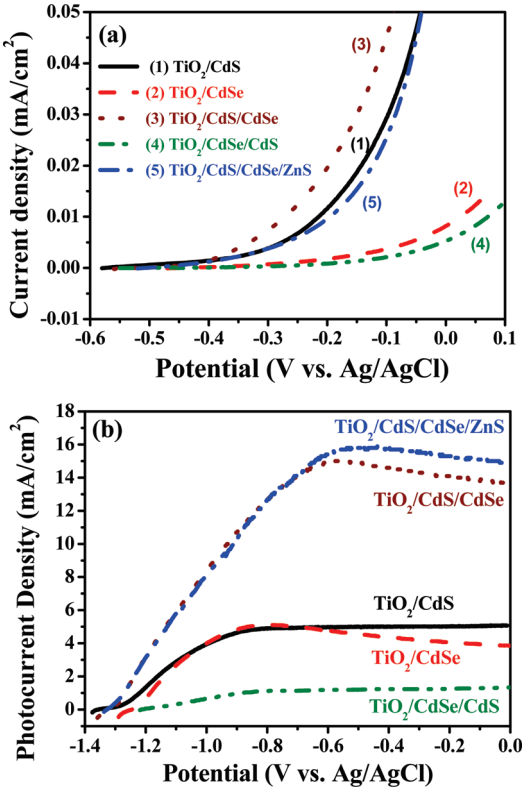

Figure 3. Current density versus potential for various photoelectrodes measured in dark conditions (a) and under illumination of AM 1.5 light (with UV cutoff) at 100 mW/cm^2 (b).

that of CdS (as shown in Scheme 1a),[21] the formation of a stepwise band edge could be attributed to the alignment of Fermi level at CdS/CdSe interface.

The shift of the Fermi level of CdS and CdSe due to their contact can be qualitatively evaluated by the open circuit potentials (OCP) deduced from Figure 3a. When a semiconductor is brought into contact with a solution containing a redox couple, the Fermi levels of the semiconductor and solution will be identical after electrostatic equilibrium. The OCP of an electrode measured in dark conditions is equivalent to this equilibrium Fermi level. The OCP measured for the TiO_2/CdS (−0.58 V, vs Ag/AgCl) is higher than that for TiO_2/CdSe (−0.46 V), implying that CdS has a higher Fermi level in comparison with CdSe. When the CdS/CdSe junction is formed, electrons will flow from CdS to CdSe until a new electronic equilibrium is approached, where the Fermi energy of the electrons in the CdS is equal to that in CdSe. The new established Fermi level should locate between those of CdS and CdSe before contact. This inference in sustained by the OCP measured for TiO_2/CdS/CdSe (−0.53 V) and TiO_2/CdSe/CdS (−0.5 V). The different OCP values obtained for the two cascade structures is ascribed to the different equilibrium states of the electrode with the electrolyte.

Generally, the flatband potential of an electrode can be determined by capacitance measurement of the electrode/electrolyte interface with the help of the Mott−Schottky plot.[26] Figure 4 shows the Mott−Schottky plot measured

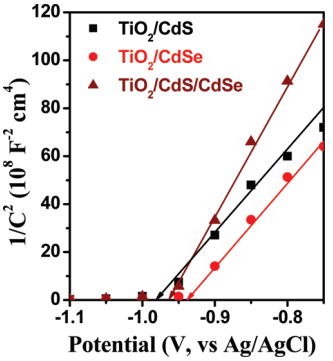

Figure 4. Mott−Schottky plots for various photoelectrodes measured at an AC frequency of 1000 Hz.

at an AC frequency of 1000 Hz for various electrodes. The flatband potentials measured from the intercept of this plot are −0.98 and −0.94 V (vs Ag/AgCl), respectively, for TiO_2/CdS and TiO_2/CdSe electrodes. For the TiO_2/CdS/CdSe electrode, an intermediate value (−0.96 V) was estimated, indicating that the flatband potential of CdSe is elevated due to its contact with CdS. This result sustains the inference that Fermi level alignment occurs between CdS and CdSe layers. It is noteworthy that in the Mott−Schottky plot, the straight line corresponding to the TiO_2/CdS/CdSe electrode has the highest slope, which implies the lowest resistance of this electrode to the charge transport.[27] This result is consistent with the highest dark current measured for the TiO_2/CdS/CdSe electrode shown in Figure 3a.

The Fermi level alignment causes downward and upward shifts of the band edges, respectively, for CdS and CdSe and, furthermore, results in a band bending and space-charge layer on each side of the junction. The band edges of CdS and CdSe before and after contact in the dark are schematically illustrated in Figure 5a,b, respectively. The conduction band of CdSe lies above that of CdS after the alignment. According to this result, the relative band edge levels of TiO_2, CdS, and CdSe in the TiO_2/CdS/CdSe and TiO_2/CdSe/CdS electrodes are deduced and shown in Figure 5c,d, respectively. The stepwise structure of TiO_2/CdS/CdSe is responsible for the higher dark current at positive bias. On the other hand, the band edges of the intermediate CdSe layer lie above that of CdS in the TiO_2/CdSe/CdS electrode (Figure 5d), which triggers a high resistance for the transfer of electrons and holes across the composite layer.

Figure 3b shows the photocurrent density versus measured potential ($I-V$) curves for the QD-sensitized TiO_2 electrodes. These measurements were performed under illumination of AM 1.5 (with UV cutoff) at 100 mW/cm^2. Because the UV light was filtered out from the illumination, the photocurrent density measured for the bare TiO_2 electrode is negligible (not shown here). For the QD-sensitized electrodes, the photocurrents demonstrate a strong dependence on the structure of the photoelectrodes. When only CdS or CdSe was used as sensitizer, the saturated current densities are 4.9 and 5.1 mA/cm^2,

(26) Mollers, F.; Tolle, H. J.; Memming, R. *J. Electrochem. Soc.* **1974**, *121*, 1160.

(27) Yoon, K. H.; Shin, C. W.; Kang, D. H. *J. Appl. Phys.* **1997**, *81*, 7024.

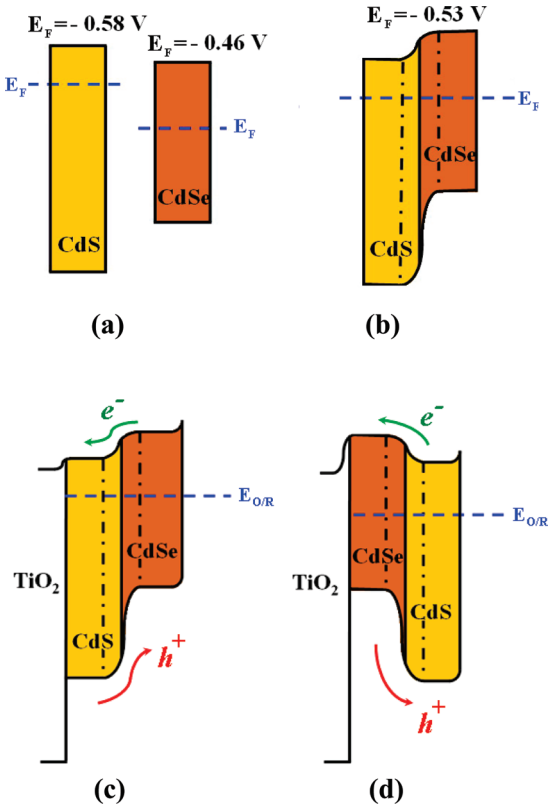

Figure 5. Relative Fermi level and band edge positions of CdS and CdSe before (a) and after Fermi level alignment due to their contact (b). The proposed band edges structures for the TiO_2/CdS/CdSe (c) and TiO_2/CdSe/CdS (d) electrodes in equilibrium with the redox couples in the electrolyte. The Fermi levels (E_F) indicated in (a) and (b) are OCPs (vs Ag/AgCl) measured in dark conditions.

respectively. For the TiO_2/CdS/CdSe co-sensitized electrode, the saturated current density markedly increases to approximately 14.9 mA/cm^2, which is three times the value of the electrodes using a single sensitizer. On the contrary, when CdS and CdSe were inversely deposited on a TiO_2 film as a TiO_2/CdSe/CdS cascade structure, a much lower current density was obtained compared with other electrodes.

When a semiconductor is irradiated by light with energy higher than its band gap, electron−hole pairs are created. The photocurrent is not only determined by the excited amount of electron−hole pairs but also by the transport of both electrons and holes across the electrode. The stepwise band-edge structure built in the TiO_2/CdS/CdSe electrode (Figure 5c), as well as the electric field in the space-charge region, is advantageous to the electron injection and hole recovery of the system, which is responsible for the high photocurrent in the TiO_2/CdS/CdSe electrode. On the other hand, for the inverse (TiO_2/CdSe/CdS) structure, the conduction and valence band edges of intermediate CdSe are higher than those of CdS, which results in notable barriers for injecting an excited electron from the outer CdS layer and transferring a hole out of inner CdSe. Significant recombination of electron and hole is expected, and, therefore, a low photocurrent is resulted in this structure.

To study the performance of these photoelectrodes at various wavelengths, experiments were conducted to

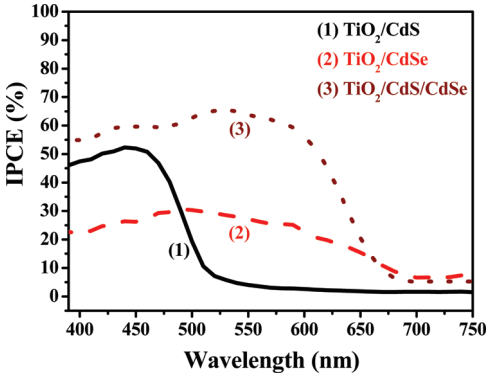

Figure 6. Incident photon to current conversion efficiencies (IPCE) for various electrodes measured from the photocurrents monitored at different excitation wavelengths. These measurements were performed at an applied voltage of 0.5 V (vs OCP).

obtain the incident photon to current conversion efficiencies (IPCE). These measurements were performed at an applied voltage of 0.5 V (vs OCP) (ca. −0.85 V vs Ag/AgCl), and the IPCEs were measured from the photocurrents monitored at different excitation wavelengths. The results shown in Figure 6 demonstrate that the IPCEs obtained for TiO_2/CdS and TiO_2/CdSe electrodes are about 50% and 30%, respectively. This result indicates that the electron−hole pairs excited in CdS can be separated and collected more efficiently than in CdSe, attributable to the higher conduction band edge of CdS compared to that of CdSe. The CdS-modified electrode only responds to the light with wavelength smaller than approximately 520 nm, while the photoactive region extends to about 680 nm for the TiO_2/CdSe electrode. For the co-sensitized electrode, TiO_2/CdS/CdSe, the light harvest region is similar to that of TiO_2/CdSe, but a much higher IPCE (ca. 60%) is obtained compared to both the CdS- and CdSe-sensitized electrodes. In the short-wavelength region (< 520 nm), the higher IPCE of TiO_2/CdS/CdSe can be attributed to the contribution of both CdS and CdSe in the light harvest. In the long-wavelength region where only CdSe can be photoexcited, the higher IPCE of the TiO_2/CdS/CdSe electrode indicates that the introduction of CdS between TiO_2 and CdSe is helpful for the collection of excited electrons from CdSe to TiO_2. This result provides additional evidence to the inference that the composite electrode (TiO_2/CdS/CdSe) constructs a band edge structure which is advantageous to the charge transport and separation of electron−hole pairs in the CdSe layer.

It was reported that ZnS can be used as a passivation layer to protect CdS and CdSe QDs from photocorrosion.[18,28] Therefore, ZnS is coated on the TiO_2/CdS/CdSe, and the electrode is denoted as TiO_2/CdS/CdSe/ZnS. The $I-V$ curve of this electrode is also shown in Figure 3. Figure 3a shows that the introduction of ZnS triggers a decrease of dark current which sustains the passivation effect of ZnS on theses materials. Under light illumination, the ZnS layer can prevent the recombination of excited electrons to the

(28) Yang, S. M.; Huang, C. H.; Zhai, J.; Wang, Z. S.; Jiang, L. *J. Mater. Chem.* **2002**, *12*, 1459.

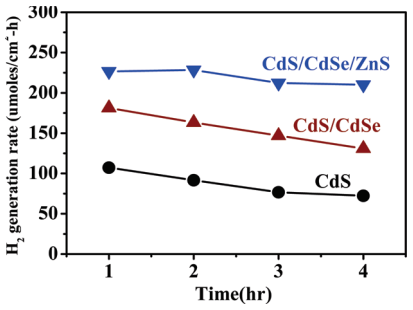

Figure 7. Variation of hydrogen evolution rates with the operation time for various QD-sensitized TiO_2 photoanodes. The photoelectrodes have a working area of 1 cm^2 and were illuminated by UV cutoff AM 1.5 light at 100 mW/cm^2.

oxidized species in the electrolyte. Therefore, the photocurrent increases slightly due to the presence of ZnS.

The electrochemical cells were used for hydrogen generation performed at the potential corresponding to the maximum efficiency (ca. −0.85 V vs Ag/AgCl). The hydrogen evolved from Pt cathode was collected and analyzed using a gas chromatograph. Figure 7 shows the hydrogen generation rate as a function of time within four hours. In the first hour, the hydrogen evolution rates for TiO_2/CdS, TiO_2/CdS/CdSe, and TiO_2/CdS/CdSe/ZnS electrodes are 107, 185, and 226 μmol cm^{-2} h^{-1}, respectively. The hydrogen generation rate of the co-sensitized electrode is much higher than the electrode using single sensitizer. Furthermore, the electrode with ZnS layer has a much higher evolution rate which not only caused by the higher photocurrent observed for the TiO_2/CdS/CdSe/ZnS electrode but also the higher stability of this electrode due to the passivation effect of ZnS. It is noteworthy that, for the electrodes without ZnS (TiO_2/CdS and TiO_2/CdS/CdSe), the hydrogen evolution rate steadily decreases with the operation time, ascribed to the photocorrosion of these electrodes. At the presence of ZnS, the evolution rate keeps nearly constant in the first two hours and decreases only slightly in the later hours. The mean hydrogen generation rate of the TiO_2/CdS/CdSe/ZnS electrode within four hours is approximately 220 μmol/(cm^2 h) (5.4 mL/(cm^2 h)). By normalizing this rate to the incident power (100 mW/cm^2), a hydrogen generation rate of 2200 μmol h^{-1} W^{-1} was achieved. To the best of our knowledge, this hydrogen generation rate is the highest among those reported for a photoelectrochemical cell under the illumination of visible light.

Conclusion

The present results show that the photoconversion efficiency of a QD-sensitized photoelectrode can be greatly enhanced by co-sensitization of CdS and CdSe, organized as a cascade structure of TiO_2/CdS/CdSe. In this electrode, the Fermi level alignment between CdS and CdSe causes downward and upward shifts of the band edges, respectively, for CdS and CdSe. Therefore, the band edges of the three materials form a stepwise structure which is advantageous to the transport of excited electrons and holes across the composite electrode. A hydrogen generation rate as high as 220 μmol/(cm^2 h) was achieved under 100 mW/cm^2 illumination of visible light.

Acknowledgment. The support of this research by the National Science Council of Taiwan through Grant NSC-96-ET-7-006-001-ET and NSC-95-2218-E-006-049 is gratefully acknowledged.